

Phase Transition of Confined Gold Nanoparticles: Replica Exchange Molecular Dynamics Study[†]

Hyunsik Kim, Feng-Yin Li,[‡] and Soonmin Jang*

Department of Chemistry, Institute for Chemical Biology, Sejong University, Seoul 143-747, Korea

*E-mail: sjang@sejong.ac.kr

[‡]Department of Chemistry, National Chung Hsing University, Taichung, Taiwan 402

Received December 5, 2011, Accepted January 5, 2012

The classical molecular dynamics simulation was used to study the phase transition of gold nanoparticles under confinement using Sutton-Chen (SC) potential. Metal gold nanoparticles with different number of atoms are subject to replica exchange molecular dynamics simulation for this purpose. The simulation showing the solid-to-liquid melting temperature largely remains unaffected by confinement, while the confinement induces characteristic pre-melting at very low temperature depending on atom number in nanoparticles.

Key Words : Gold nanoparticle, Molecular dynamics simulation, Confinement

Introduction

The physical and chemical properties of nanoparticles are very different from that of the bulk matter mainly due to large surface-to-volume ratio and highly depend on its size.¹ The melting behavior, i.e. solid to liquid phase transition, of metal nanoparticles also exhibit size dependent features. One of the most extensively studied metals for this purpose is sodium (both in charged and neutral shapes). Also, aluminum clusters were subject to intensive study for the same purpose.² Generally, the melting point of the metal cluster decreases as the cluster size decreases, but this trend is not always monotonous. For example, the melting temperature of sodium nanoparticles fluctuates in cluster of particle number from 55 to 200 atoms.³ In some cases, the melting temperature of nanocluster is higher than that of bulk metal.⁴

Gold nanoparticles have been subject of intensive research for variety of applications due to characteristic optical and electrical properties. The phase transition of nano-sized gold clusters has been studied both experimentally and theoretically. Experimental measurement of nanoparticle phase transition involves calorimetric measurement of heat capacity change due to latent heat and ion mobility measurement. Dick *et al.*⁵ have measured the melting temperature of silica-encapsulated gold nanoparticles of several different sizes. They have shown that the melting temperature decreases sharply as the particle size decreases. Sometimes, the metal nanoparticles show melting at more than single temperature, leading pre-melting or post-melting. The pre-melting refers to the phase change at lower temperature than the solid-to-liquid melting temperature, while the post-melting refers to the phase change at higher than the melting temperature. This is because the thermodynamics behaviors of atoms at cluster shell and the atoms at cluster core are different, and only shell regions or

core regions melted under certain conditions.² In some cases, the pre-melting involves the solid-to-solid phase transition.⁶

Unlike experiment, molecular dynamics simulation gives detailed structural information as well as thermodynamic values, providing excellent opportunities to understand the phase transition under the simulation condition. Usually, at least several nanoseconds of simulation time is needed to evaluate the melting temperature of metal nanoparticles, and even this simulation might suffer from broken ergodic problem, i.e. lack of enough canonical sampling at given temperature.² This difficulty could be not as severe as other complex molecular systems, such as biomolecular system. But this has to be properly handled if the simulation length is not long enough.

Unlike the metal nanoparticles in vacuum, the melting behavior of metal nanoparticles under the geometrically confined space may show somewhat different features, and both the theoretical and experimental studies under the confinement are largely unexplored. The metal clusters inside carbon nanotubes (CNTs) and zeolite-encaged catalytically active transition metals are examples of metal nanoparticles under confinement.⁷ The purpose of current simulation is investigation of phase transition under confinement. In this paper, we have studied the phase transition of gold nanoparticles with around 38 atoms under the confined space. The gold has *fcc* structure, and the nanoparticle has icosahedral structure when it has specific number of atoms, called the magic number.⁸ The smallest magic number is 38. We have studied the phase transition of gold metal clusters with 36, 37, and 38 atoms using molecular dynamics simulation. We have employed the replica exchange molecular dynamics (REMD) simulation⁹ to enhance the overall simulation efficiency mentioned above. Mainly, we have estimated the constant volume heat capacity as a function of different temperature to monitor the phase change of gold nanoparticles, and the resulting thermodynamic and structural features are discussed.

[†]This paper is to commemorate Professor Kook Joe Shin's honourable retirement.

Methods

In REMD, several independent trajectories at different temperature are propagated simultaneously. Then, the trajectories between each neighboring temperatures are exchanged at every given interval. This introduces the stochastic jump into current trajectory, enabling efficient sampling of overall energy landscape while maintaining the canonical energy distribution at simulation temperature. As for potential energy, we have the semi-empirical Sutton-Chen (SC) potential for metals.¹⁰ It has the following energy form.

$$U = \varepsilon \sum_{i=1}^N \left[\sum_{j \neq i}^N \frac{1}{2} \left(\frac{a}{r_{ji}} \right)^n - c \sqrt{\rho_i} \right]$$

where, N is the total number of atoms, $\rho_i = \sum_{j \neq i}^N (a/r_{ji})^m$, and r_{ij} is distance between atom i and j . The potential parameters c , m , and n are optimized to fit the properties such as cohesive energy and bulk modulus. The remaining parameters ε and a are energy depth and length parameter, respectively. The parameter is given in Table 1. Note that the total energy is not pairwise interaction. The first term is repulsion energy, and the second term represents the many-body cohesion energy. The resulting expression of force, negative gradient of potential, with respect to atom i along the x -direction is given as

$$-\left(\frac{\partial U}{\partial x_i}\right) = \left[n\varepsilon \sum_{j \neq i} \left\{ n\varepsilon \left(\frac{a}{r_{ji}} \right)^n \frac{(x_i - x_j)}{r_{ji}^2} \right\} \right] - \frac{c\varepsilon m}{2} \left\{ \frac{1}{\sqrt{\rho_i}} \sum_{j \neq i}^N \left[\left(\frac{a}{r_{ji}} \right)^m \frac{(x_i - x_j)}{r_{ji}^2} \right] + \sum_{j \neq i} \left[\frac{1}{\sqrt{\rho_i}} \left(\frac{a}{r_{ji}} \right)^m \frac{(x_i - x_j)}{r_{ji}^2} \right] \right\}$$

The number of replica was 24 with temperature range of 30 K ~ 2000 K. The simulation temperatures of 24 replicas are listed in Table 2. The initial structure for the simulation was taken as the icosahedral geometry with 38 atoms and shown in Figure 1. Indeed, our REMD simulation using 38 atoms starting from cubic lattice like structure shows this icosahedral geometry is the most stable structure, and the initial structure does not affect the overall simulation results as long as the trajectory has reached canonical equilibrium in REMD simulation. For 36 and 37 atom simulations, we deleted two and one atoms at surface, respectively.

For confinement effect, we have enclosed the gold metal clusters inside the sphere with reflecting boundary condi-

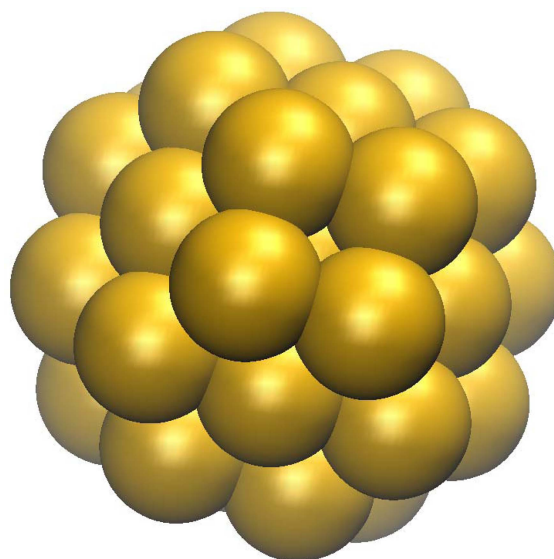


Figure 1. The most stable icosahedral structure of gold nanoparticle with 38 atoms.

tion.¹¹ We have performed simulation at several different sphere sizes. The spheres radiuses are 6.0 Å, 6.1 Å, 6.5 Å, 7.0 Å, and 8.0 Å. The phase transition under this confinement environment might show distinct pattern compared to loosely confined or confinement free metal nanoparticles.

Considering the highest temperature in REMD, 2000 K, we have used rather small molecular dynamics time step of 0.25 fs to ensure the trajectory stability in our simulation. The total time step we have used is 4×10^6 , resulting in 1.0 ns for each replica. The Verlet algorithm was used for time integration, and the temperature was controlled using Nose-Hoover thermostat of chain length two.¹² Each atom has its own thermostat in our simulation. The replica exchange was attempted at every 50 fs. The structure was saved at every 1000 steps, and the energy was written at every 200 steps for further analysis.

We have estimated the constant volume heat capacity c_v from the energy fluctuation

$$c_v = \frac{1}{k_B T^2} [\langle E^2 \rangle - \langle E \rangle^2],$$

where k_B is Boltzmann's constant and T is temperature.

We have discarded initial 0.25 ns of simulation trajectory in our heat capacity calculation to ensure the convergence of simulation. The final heat capacities are obtained from four independent simulations.

Results and Discussions

The overall replica exchange acceptance ratio was about 32 % for all three systems. We have traced replica exchange as a function of simulation time during REMD simulation, which is shown in Figure 2 for replica 1 (black) and 2 (red) corresponding to initial temperatures of 30 K and 2000 K, respectively. The figure was obtained for simulation with 38

Table 1. Sutton-Chen potential parameters for gold metal

a (Å)	ε (10^{-2} eV)	c	m	n
4.08	1.27930	34.408	8	10

Table 2. The simulation temperatures of 24 replicas (in Kelvin)

30	36	42	52	63	78	95	120
150	185	227	275	321	370	428	495
575	675	810	970	1150	1360	1640	2000

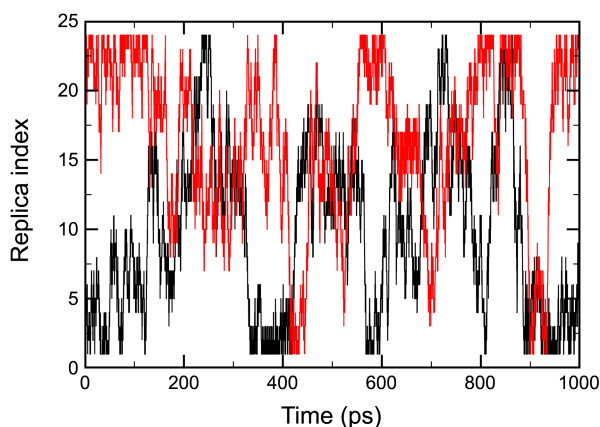


Figure 2. The time profile of exchange history of two replicas. Other replicas show similar behavior.

atoms and sphere radius of 6.5 Å. Other replicas with different atom number and different sphere radius show similar behavior. A single trajectory visits all replica indexes frequently during the simulation time, indicating that the system shows reasonable stochastic mixing of different replicas.

The temperature dependent constant volume heat capacities of three different system sizes are shown in Figure 3. The heat capacities at different sphere radius are indicated in separate panels. Essentially, the heat capacities have three main peaks. The first peak has broad shape around 700 K, and the second peak appears at from 220 K to 300 K depending on the sphere radius and system size. These second peaks are relatively sharp compare to the first peak. Finally, at around 100 K, there is very sharp peak. The first peak must have corresponds to the melting of the whole nanoparticle in each case. In fact, the experimental study of Dick *et al.* indicates the melting temperature of 15 Å silica-encapsulated gold nanoparticle is 380 °C (653 K),⁵ which is

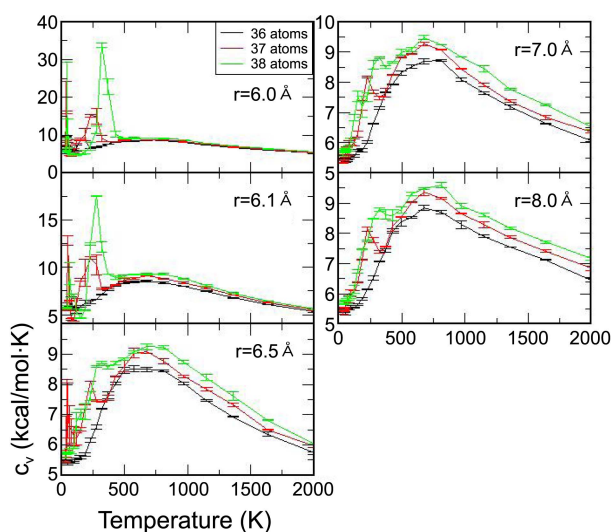


Figure 3. The constant volume heat capacities evaluated from current REMD simulation at various temperatures. Heat capacities under the different confining sphere radius are indicated on different panel.

close to the melting temperature obtained from current simulation (~ 700 K), even though the system size is somewhat different. At least within the current system size variation of 36, 37, and 38 atoms, this melting temperature change is minimal. The second peaks, peaks around 220 K \sim 300 K, correspond to the solid-to-solid pre-melting.² The molecular dynamics simulation trajectory at 275 K for 38 atoms with confining sphere radius of 6.1 Å shows two distinct solid-like structures, which are shown in Figure 4. No other structures are observed other than these two structures at this temperature. This clearly indicates the current pre-melting is associated with the structural transition between two different structures. This pre-melting solid-to-solid phase transition is less pronounced as the confinement radius is increase, i.e. as the system is loosely confined. Nevertheless, it still survives despite being under the very weak confinement for 37 and 38 atoms. Also, it is noted that this pre-melting temperature is essentially unaffected by the confinement.

Finally, it can be seen that the peak at around 100 K quickly disappears as the confinement space is increased. This peak is observed in any other molecular dynamics simulations. Therefore, the sharp phase transition at around 100 K must be due to confinement. To investigate the structural change responsible to this phase transition, we have monitored the trajectory at 97 K with 38 atoms under the confinement radius of 6.5 Å. The number of different structures observed at this temperature is also only two. One is the icosahedral structure, the most stable structure, and the other is shown in Figure 5. In other words, the confinement induces phase transition at low temperature, lower than the pre-melting temperature, between the most stable icosahedral structure and the structure shown in Figure 5. Unlike 37 and 38 atom nanoparticles, the nanoparticle with 36 shows somewhat different behavior. Notably, it has no pre-melting under the confinement free condition, or very weak confinement, but the pre-melting begins to show as the system is subject to the high confinement. This is an indication of the discrete nature of nanoparticles, i.e. the nanoparticle properties are not monotonous functions of the system size.²

In summary, depending on the system size, the confinement of metal gold nanoparticles induces pre-melting or yet another phase transition at low temperature. The quantum

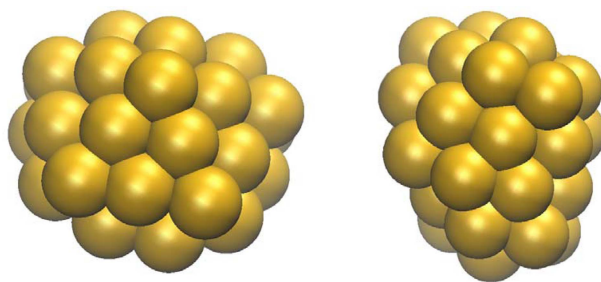


Figure 4. The 38 atom gold nanoparticle structures at 275 K when the confining sphere size is 6.5 Å. Only these two structures can be observed at this temperature, which corresponds to the pre-melting temperature.

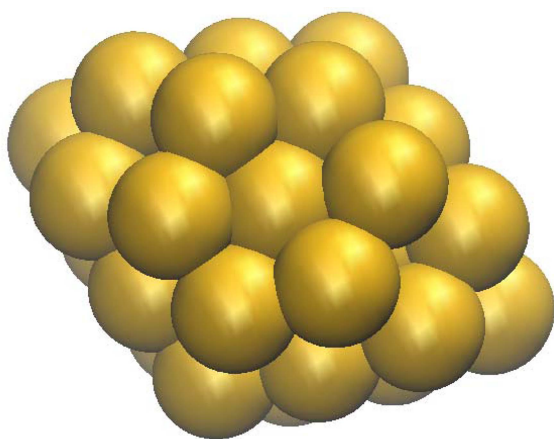


Figure 5. The 38 atom gold nanoparticle structures at 95 K when $r = 6.5$ Å. Only this structure and icosahedral structures are observed at this temperature.

simulations of some metal nanoparticles with DFT based potential energy are reported.⁸ But systematic simulation of phase transition using quantum potential energy is not easily feasible. The current classical simulation could provide a qualitative aspect of phase transition, especially phase transition under the confinement. In the current study, we have not performed the detailed structural analysis, such as the order parameter¹³ and radial distribution of the resulting trajectories, which could provide additional insight into metal nanoparticle phase transitions. Recently, the metal alloy nanoparticle has attracted considerable interest as a novel catalyst. Combined with suitable analysis, we believe the extension of current simulation strategy to these metal nanoparticles should provide valuable information on structural and thermodynamic properties of nano-sized metal particles.

Acknowledgments. This work was supported by the National Research Foundation of Korea (NRF) grant funded by the Korean government (No. 2009-0068898 & No. 2010-0015536). The simulation was performed at the Supercom-

puting Center (Strategic Supercomputing Support Program) at Korea Institute of Science and Technology Information (KISTI).

References

1. Baletto, F.; Ferrando, R. Structural Properties of Nanoclusters: Energetic, Thermodynamic, and Kinetic Effects. *Rev. Mod. Phys.* **2005**, *77*, 371.
2. Aguado, A.; Jarrold, M. F. Melting and Freezing of Metal Clusters. *Annu. Rev. Phys. Chem.* **2011**, *62*, 151.
3. Haberland, H.; Hippler, T.; Donges, J.; Kostko, O.; Schmidt, M.; von Issendorff, B. Melting of Sodium Clusters: Where do the Magic Numbers Come From? *Phys. Rev. Lett.* **2005**, *94*.
4. Breaux, G. A.; Benirschke, R. C.; Sugai, T.; Kinneer, B. S.; Jarrold, M. F. Hot and Solid Gallium Clusters: Too Small to Melt. *Phys. Rev. Lett.* **2003**, *91*.
5. Dick, K.; Dhanasekaran, T.; Zhang, Z. Y.; Meisel, D. Size-dependent Melting of Silica-encapsulated Gold Nanoparticles. *J. Am. Chem. Soc.* **2002**, *124*, 2312.
6. Van Hoof, T.; Hou, M. Structural and Thermodynamic Properties of Ag-Co Nanoclusters. *Phys. Rev. B* **2005**, *72*.
7. (a) van der Klink, J. J.; Brom, H. B. NMR in Metals, Metal Particles and Metal Cluster Compounds. *Prog. Nucl. Mag. Res. Sp.* **2000**, *36*, 89; (b) Deepak, J.; Pradeep, T.; Waghmare, U. V. Interaction of Small Gold Clusters with Carbon Nanotube Bundles: Formation of Gold Atomic Chains. *J. Phys.-Condens. Mat.* **2010**, *22*.
8. Barnard, A. S. Modelling of Nanoparticles: Approaches to Morphology and Evolution. *Rep. Prog. Phys.* **2010**, *73*.
9. Sugita, Y.; Okamoto, Y. Replica-exchange Molecular Dynamics Method for Protein Folding. *Chem. Phys. Lett.* **1999**, *314*, 141.
10. Sutton, A. P.; Chen, J. Y. Long-range Finnis-Sinclair Potentials. *Philosophical Magazine Letters* **1990**, *61*, 139.
11. Mo, Y. X.; Lu, Y.; Wei, G. H.; Derreumaux, P. Structural Diversity of the Soluble Trimers of the Human Amylin (20-29) Peptide Revealed by Molecular Dynamics Simulations. *J. Chem. Phys.* **2009**, *130*.
12. Martyna, G. J.; Klein, M. L.; Tuckerman, M. E. Nose-Hoover Chains: The Canonical Ensemble via Continuous Dynamics. *J. Chem. Phys.* **1990**, *97*, 2635.
13. Yang, Z.; Yang, X. N.; Xu, Z. J. Molecular Dynamics Simulation of the Melting Behavior of Pt-Au Nanoparticles with Core-shell Structure. *J. Phys. Chem. C* **2008**, *112*, 4937.